

FACTA UNIVERSITATIS

Series: **Electronics and Energetics** Vol. 28, N° 4, December 2015, pp. 585 - 596

DOI: 10.2298/FUEE1504585C

## NUMERICAL CALCULATION OF SHIELDING EFFECTIVENESS OF ENCLOSURE WITH APERTURES BASED ON EM FIELD COUPLING WITH WIRE STRUCTURES

**Tatjana Cvetković<sup>1</sup>, Vesna Milutinović<sup>1</sup>,  
Nebojša Dončov<sup>2</sup>, Bratislav Milovanović<sup>3</sup>**

<sup>1</sup>Regulatory Agency for Electronic Communications and Postal Services, Belgrade, Serbia

<sup>2</sup>Faculty of Electronic Engineering, University of Niš, Niš, Serbia

<sup>3</sup>Singidunum University of Belgrade, Belgrade, Serbia

**Abstract.** *Shielding effectiveness of a protective metal enclosure with apertures and receiving antenna placed inside is numerically considered. The purpose of the antenna, here considered as a dipole, is to detect the electromagnetic (EM) field level within the enclosure and to transfer this information via a coaxial cable to a network analyzer. This follows the experimental procedure used to measure the shielding effectiveness of enclosure. A numerical model, based on the Transmission-Line Matrix (TLM) method enhanced with so-called wire node, is used to simulate this dipole antenna/cable arrangement in order to investigate how much it disturbs the level of shielding effectiveness due to their two-way coupling with EM field inside the enclosure. The numerical model, whose accuracy is proved by comparison with experimental results available in the literature, is used to consider the influence of radius and length of the dipole-receiving antenna and the impact of cable presence on the distribution of EM field inside the enclosure and shift of resonant frequencies for normal and oblique incidence.*

**Key words:** *Enclosure, apertures, shielding effectiveness, TLM method, dipole-receiving antenna, coaxial cable*

### 1. INTRODUCTION

Many factors can influence an electronic system behavior in terms of electromagnetic compatibility (EMC) [1]. The character and importance of electromagnetic (EM) radiation from different parts of the system and the impact of interference, generated externally, on the functional integrity of an entire system have to be considered during the system design. To provide the EM signature of equipment and immunity to electromagnetic interference (EMI) that both meet limits specified in EMC standards, a designer can seek to minimize interference at its source, reduce coupling paths by choosing a suitable layout,

---

Received November 18, 2014; received in revised form March 5, 2015

**Corresponding author:** Tatjana Cvetković

Regulatory Agency for Electronic Communications and Postal Services, Višnjićeva 8, 11000 Belgrade, Serbia  
(e-mail: [tatjana.cvetkovic@ratel.rs](mailto:tatjana.cvetkovic@ratel.rs))

apply shielding, filtering, grounding, etc. Enclosures usually built of highly conductive materials, are often used to protect the system from external EM fields but also to reduce EMI emission from equipment. Their protective characteristic is often expressed as a ratio between the field strength without and with shield at some point inside the enclosure (so-called shielding effectiveness – SE) and it can be defined both in terms of the electric and magnetic fields. EM characteristics of materials used to build the enclosure walls as well as the structure and form of the enclosure can significantly influence the value of this parameter and therefore the immunity of the whole system.

Apertures of various forms, intended for heat dissipation, insertion of control panels and outgoing or incoming cables, airing or other purposes are integral parts of the shielding enclosure. Apertures can significantly degrade the shielding performances of the enclosure as EM radiation penetrates through the apertures in the inside/outside space. Besides apertures, there is a penetration via diffusion through conducting enclosure walls [1], but it is less significant if conductivity of the walls is high. The EM energy, which penetrates into enclosure, often couples into wires, which are part of transmission lines such as printed circuit boards (PCBs) or cable, and then propagates causing further interference. Therefore, it is important to consider all these coupling mechanisms, in order to design the enclosure with satisfying SE over the frequency range of interest. There are many methods which can be used for the calculation of the SE. Some of them are analytical methods [2-4] that can be very efficient but with some limitations. For an example an equivalent waveguide circuit proposed in [3,4] was developed to tackle normal [3] and oblique incidence and arbitrary location of apertures on the enclosure walls [4], but only in the case of an empty enclosure. Numerous numerical methods are also often used for the SE calculation, e.g. the finite difference time domain (FDTD) method [5], the methods of moments (MoM) [6] and the transmission line matrix (TLM) method [7-10]. They are generally applicable to complex problems, usually without any limitations but with high computational cost. In addition to that, once the enclosure is made off, measurements can be conducted for determination of its SE. To measure the level of EM field as some critical points inside the enclosure, a receiving antenna such as monopole [3] or dipole [4] can be used, while the coaxial cable transfers the induced current/voltage information to an instrument that records measurement results (network analyzer, spectrum analyzer, EMC receiver).

In [11-13] authors have numerically consider the impact of the physical presence of the receiving dipole antenna on the level of EM field inside the enclosure and therefore on accuracy of estimated SE when antenna is used in an experimental procedure. The motivation for this research was that equivalent circuitual model presented in [4] provided SE results slightly different from the measurements due, as stated in [4], its inability to include the receiving antenna. Also, some of the authors of this paper have been previously shown that antenna placed inside the microwave cavity can influence the EM field distribution and location of resonant frequencies [14]. The TLM method incorporating the compact wire model, developed in [15] and adapted in [16] for cylindrical mesh, has been used to create a numerical model capable of taking into account the antenna presence. In addition, in [12] the equivalent circuitual model proposed in [3,4] has been extended to include the receiving antenna. Due to numerical model ability to account, unlike circuitual model, for two-way interaction between EM field inside the enclosure and receiving dipole antenna, we proceed in this paper with using only the numerical model in our analysis of wire parameters impact on the SE. Besides directly sampling the EM field in

the space nearby antenna to estimate the SE of enclosure as in [11,12], another way of collecting signal that corresponds to the experimental procedure is also proved to be valid [13]. A current signal can be picked up directly from the antenna and then used to find the voltage induced in the center of the dipole antenna to calculate the SE.

In this paper, the numerical model is applied on a rectangular enclosure with three different aperture patterns on the front wall and comparison with measurement SE results [4] is provided. An analysis of wire radius and length influence on the level of SE of enclosure and location of resonant frequencies, more detailed than one conducted in [13], is presented here for the case of plane wave of normal incidence and with horizontal polarization. In addition, an oblique incident plane wave defined by appropriate azimuth, elevation and polarization angles is used as an excitation in order to demonstrate how placing antenna in three different positions to detect each field component significantly influences the detected level of the SE. Signal transfer to the measurement instrument via a coaxial cable is taken into account by directly modeling the cable in the numerical model. Its impact on the SE is illustrated for a plane wave of normal or oblique incidence to the frontal panel and with horizontal or arbitrary electric polarization.

## 2. TLM METHOD ENHANCED WITH WIRE NODE DESCRIBING ENCLOSURE WITH APERTURES AND RECEIVING ANTENNA INSIDE

The TLM method [17] is a differential time-domain numerical technique based on temporal and spatial sampling of EM fields. The fundamental building block in the TLM method is known as the symmetrical condensed node (SCN) consisting of 12 interconnected link lines (Fig. 1) that model a cuboid piece of space ( $\Delta x \times \Delta y \times \Delta z$ ). The network of interconnected SCNs, together with chosen parameters of link lines, is used here to describe the EM properties of a medium inside/outside the enclosure. In addition, short and open stubs (not shown in Fig. 1a) can be attached to SCNs to model inhomogeneous and lossy materials.

Imperfectly conducting enclosure walls are modeled by terminating the TLM link lines at the edge of the enclosure space with an appropriate load. Cross-section of each aperture on an enclosure wall is described by using a fine TLM mesh so that there are several nodes across aperture width and length. Aperture depth is also taken into account by using a few nodes across wall thickness. In the case of an array of apertures on enclosure walls (e.g. for ventilation purposes), a compact air-vent model [8] is proved to be more efficient, while in the case of slots (apertures whose length is significantly larger than dimensions across the slot) a compact slot model can be used [9].

Regarding the wire structures inside the enclosure, the most efficient solution is to use a compact wire model consisting of additional wire network, formed by two link lines and one short-circuit stub line, embedded within SCN (so-called wire node, Fig. 1b). As wire node model one wire segment, a column of nodes is usually required to model the whole wire length. This model allows for accurate modeling of wires having a considerably smaller diameter than the node size (up to 40% of node cross-section size). In addition, it models signal propagation along the wires, while allowing for interaction with the external EM field (two-way interaction). Wire presence increases the capacitance and inductance of the medium in which they are placed so characteristic impedance parameters of link and stub lines,  $Z_{wi}$  and  $Z_{wsi}$ ,  $i \in (x, y, z)$ , respectively, have to be chosen to model this increase in

capacitance and inductance in the direction of wire axis, maintaining at the same time synchronism with the rest of the transmission line network.

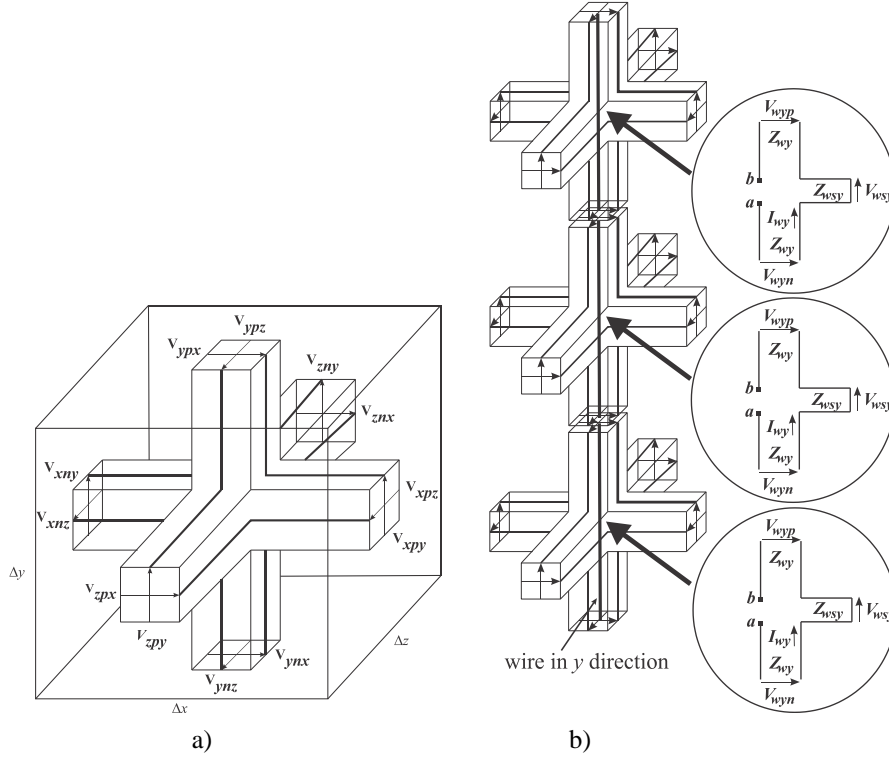


**Fig. 1** a) Symmetrical condensed node (SCN), b) a column of wire nodes (SCNs with additional wire networks - two link lines and one short-circuit stub line per node model one wire segment)

For example, in the case of wire running in  $y$  direction, the characteristic impedances of link and stub lines can be expressed as:

$$Z_{wyy} = \frac{\Delta t}{\Delta y C'_w}, \quad Z_{wsy} = L'_w \frac{\Delta y}{\Delta t} - Z_{wyy} \quad (1)$$

where  $\Delta y$  represents the dimension of the TLM node in the direction of the wire segment passing through the node,  $\Delta t$  is a time-step discretization,  $C'_w$  and  $L'_w$  are the wire capacitance and inductance per-unit length, respectively, calculated as:

$$C'_w = 2\pi\epsilon / \ln(k_{Ci}\Delta y_c / r_w), \quad L'_w = \mu \ln(k_{Li}\Delta y_c / r_w) / 2\pi \quad (2)$$

where  $\Delta y_c$  represents mean cross-section dimensions of the TLM node in the  $y$  direction,  $\Delta y_c = (\Delta x + \Delta z) / 2$ ,  $r_w$  is the wire radius and  $k_{Ci}$  and  $k_{Li}$  are factors obtained empirically by using the known TLM network characteristics and the mean dimensions of the node cross-section in the wire running direction [15].

The current in a straight wire segment running in the  $y$  direction can be found as [15]:

$$I_{wy} = \frac{2(V_{wyz}^i + 2V_{wzy}^i - 2V_{wyp}^i - V_{ab}^i)}{2Z_{wy} + Z_{wzy} + Z_{ab}}, \quad (3)$$

where  $V_{ab}$  and  $Z_{ab}$  describe the two-way coupling of the link lines of SCN polarized in the  $y$  direction (pulses  $V_{xny}$ ,  $V_{xpy}$ ,  $V_{zny}$  and  $V_{zpy}$  and characteristic admittances  $Y_{xy}$  and  $Y_{zy}$ ) and open circuit stub of SCN polarized in the  $z$  direction (pulse  $V_{oy}$  and characteristic admittance  $Y_{oy}$ ) with the additional wire network [17]:

$$V_{ab} = \frac{2(V_{xny}^i + V_{xpy}^i)Y_{xy} + 2(V_{zny}^i + V_{zpy}^i)Y_{zy} + 2V_{oy}^i Y_{oy}}{2(Y_{xy} + Y_{zy}) + Y_{oy}}, \quad (4)$$

$$Z_{ab} = (2Y_{xy} + 2Y_{zy} + Y_{oy})^{-1}. \quad (5)$$

Similar expressions per wire node can be derived for straight wire segments running in other two directions. 3D TLM<sub>scn</sub> solver, based on SCN and designed at the Microwave Lab of the Faculty of Electronic Engineering in Nis, incorporates the wire node feature allowing to efficiently model wire structures.

### 3. NUMERICAL ANALYSIS AND RESULTS

A rectangular enclosure with three different aperture patterns on the front wall (Fig. 2) is used to analyze the influence of a dipole-receiving antenna and coaxial cable connection on the SE. The dimensions of enclosure are the same as specified in [4]. It should be noted that in [4] the radius of the dipole-receiving antenna used in measurements is not specified. Externally generated interference is represented as a plane wave of normal incidence to the wall with apertures and with horizontal electric polarization ( $E_y$ ). A fine TLM mesh has been used to accurately describe the apertures cross-section and wall thickness of 2 mm in the numerical model of an empty enclosure. The similar behavior of the SE in the considered frequency range can be noticed in Fig. 3 for all three aperture patterns. The only difference is regarding the level of the SE due to different percentage of wall surface covered by apertures resulting in different amount of EM energy penetrating into the space inside the enclosure.

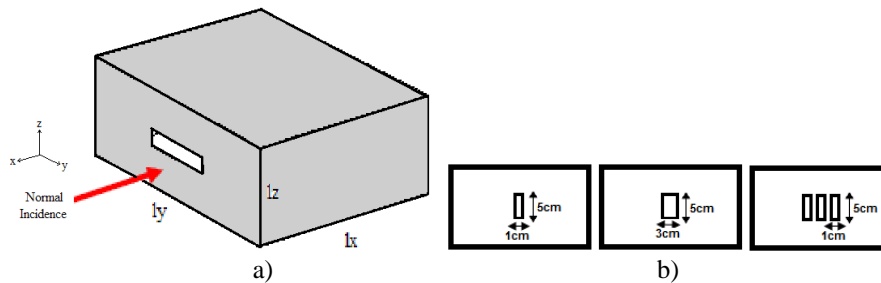


**Fig. 2** a) Enclosure of a rectangular cross-section,  
 b) front panel with one or three differently sized apertures

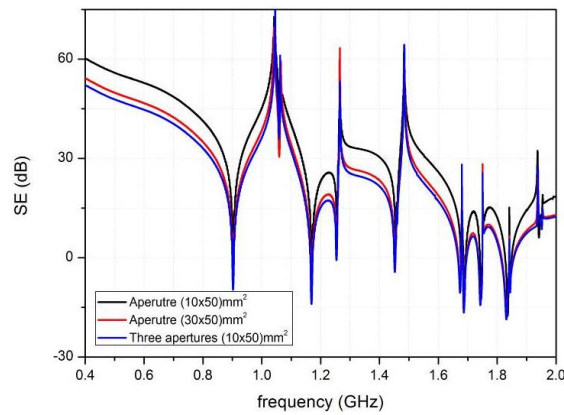


**Fig. 3** SE of enclosure with various aperture patterns on the front wall - TLM model of enclosure without antenna

Two wires, running in the  $y$  direction, each with length of 50 mm and radius of 0.1 mm, and separated by 2 mm are then used to create a receiving-dipole antenna. Wires are represented by the TLM wire node as explained in section 2. Position of both wire arms of the antenna inside the enclosure is defined according to [4]. Both wire arms are terminated by resistors in order to have the dipole antenna loaded with coaxial cable impedance. Physical presence of the coaxial cable will be modeled (discussed) later on in the paper. Balun often used between unbalanced and balanced transmission lines is not considered in this paper, but cable-antenna coupling is realized to be symmetric.

Currents induced on both wire arms of the loaded dipole antenna are of equal amplitudes and opposite signs and they can be used to find the voltage induced between the mutually nearest ends of two wires, i.e. in the center of the dipole antenna. For illustration purposes, the currents running at the terminating resistors of dipole wire arms, as well as the induced voltage, are shown in Fig. 4 for the case of the enclosure with one (10 x 50) mm<sup>2</sup> aperture on the front wall of the enclosure.

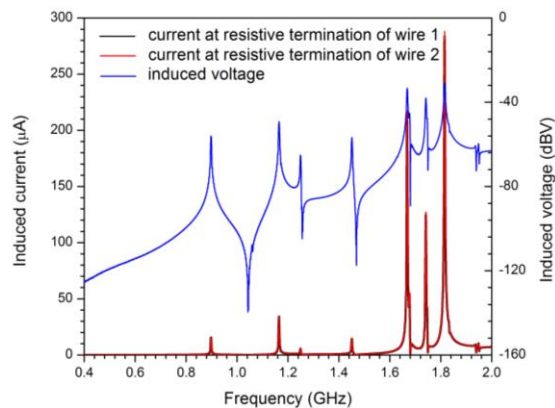


**Fig. 4** Induced currents at the terminating resistors of wire arms (overlapping black and red solid lines) and voltage induced between wire arms as a function of frequency

Numerical result for the SE obtained from the voltage difference between two arms of loaded dipole antenna, without and with the enclosure with one  $(10 \times 50) \text{ mm}^2$  aperture on the front wall, is shown in Fig. 5. It is also compared to the case when only presence of dipole antenna is taken into account (i.e. EM field is directly taken at a point in space between dipole wire arms). It can be observed that the level of SE is always lower in the case when the dipole antenna loaded with coaxial cable impedance is taken into account and that in some frequency regions TLM model with loaded antenna follows better experimental results. The similar conclusions can be reached for other two apertures patterns. However, it should be pointed out that more accurate comparison of these two TLM models with the experimental results has to include the balun presence and its characteristics in considered frequency range which was not given in [4].

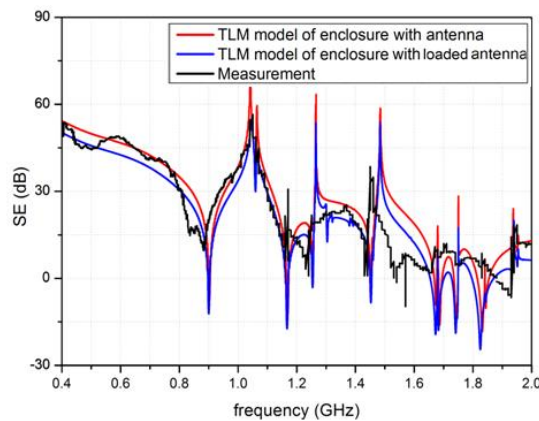


**Fig. 5** SE of enclosure with one  $(10 \times 50) \text{ mm}^2$  aperture on the front wall - TLM models of enclosure with antenna, with loaded antenna and measurements [4]

As already illustrated in [13], wires of different radius and length, used to represent receiving dipole antenna arms, can influence the SE and shift the resonant frequencies of the enclosure. At and around resonant frequencies, the level of SE can be very low indicating poor shielding so it is important to also accurately determine their values. Therefore, a more detailed analysis of antenna physical dimensions influence on the EM field distribution inside the enclosure is conducted here. The radius of the both wire arms was changed in the range (0-2) mm, while the length varied in the range (50-150) mm. Their impact on the level of SE and location of three resonant frequencies of the enclosure with one  $(10 \times 50) \text{ mm}^2$  aperture on the front wall for horizontally polarized plane wave of normal incidence is shown in Figs.6-9. Figs. 6 and 7 show how the  $\Delta\text{SE}$  varies as a function of frequency for different radii and lengths of the antenna, respectively, where  $\Delta\text{SE}$  represents difference between the level of the SE of considered enclosure in the absence and presence of dipole antenna. Thicker and longer wires affect more the level of SE in comparison with the case when antenna is not placed inside the enclosure. This impact is almost constant over the considered frequency range except around resonant frequencies where also shift of resonant frequencies has to be taken into account. Location of resonant frequencies, compared to the case on empty enclosure changes towards lower frequencies with the increase of wire

radius and length, as shown in Figs. 8 and 9, respectively, for three resonant frequencies indicated in [4]. This shift can be significant especially for thicker and longer wires and, as in the case of level of the SE, it is due to stronger influence of the antenna on the total EM field inside the enclosure.

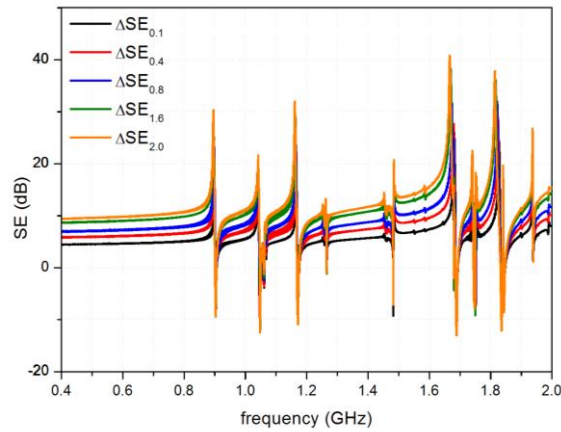


**Fig. 6** Difference between the level of the SE of enclosure with one (10x50) mm<sup>2</sup> aperture on the front wall in the absence and presence of dipole antenna with various radii and length of 100 mm

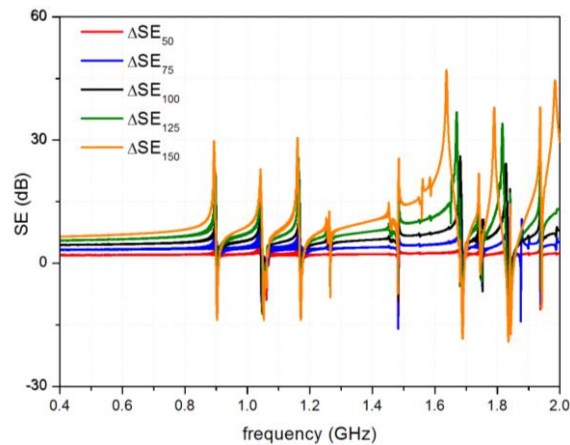


**Fig. 7** Difference between the level of the SE of enclosure with one (10x50) mm<sup>2</sup> aperture on the front wall in the absence and presence of dipole antenna with various lengths and radius of 0.1 mm



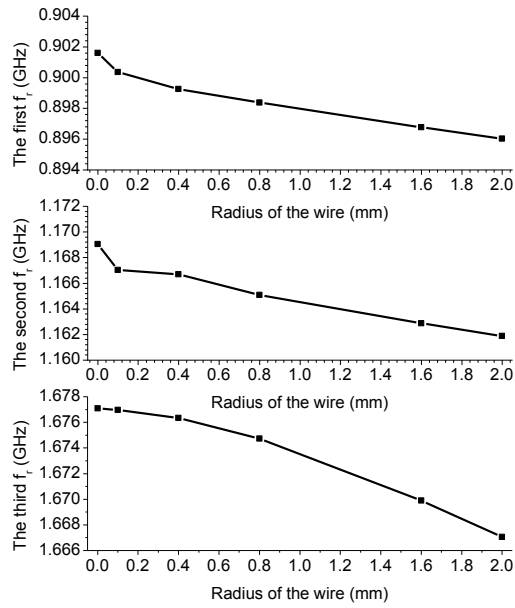


**Fig. 8** Resonant frequency of the SE of enclosure with one (10x50) mm<sup>2</sup> aperture on the front wall versus radius of the dipole antenna; antenna length is 100 mm

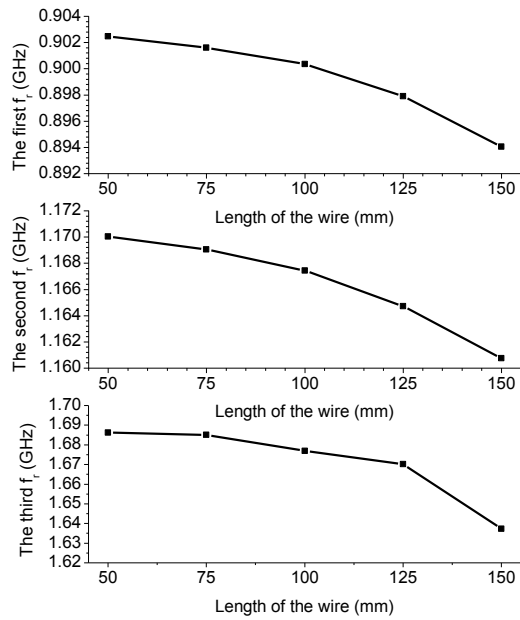


**Fig. 9** Resonant frequency of the SE of enclosure with one (10x50) mm<sup>2</sup> aperture on the front wall versus length of the dipole antenna; antenna radius is 0.1 mm

In all previously considered examples, a plane wave of normal incidence to the frontal panel and with horizontal electric polarization ( $E_y$ ) is used as an excitation. As a result, the dominant EM field component excited inside the enclosure is in the  $y$  direction and the dipole-receiving antenna has to be positioned during the measurement only in this direction in order to calculate the SE. However, in general, a plane wave can be with arbitrary incident angle and polarization so that all three EM field components can exist inside the enclosure, which requires that in the experimental procedure the dipole receiving antenna is separately placed along each of the three Cartesian axes. Therefore, the dipole antenna presence influences the detected level of each EM field component and, hence, it has a stronger impact on the accuracy of determining the total SE of the enclosure. As an illustration, the SE of the enclosure with three  $(10 \times 50)$  mm<sup>2</sup> apertures on the front wall for an obliquely incident plane wave with the azimuth angle  $60^\circ$ , elevation angle  $90^\circ$  and polarization angle  $30^\circ$  is calculated. Numerical TLM results for the case of an empty enclosure (without dipole-receiving antenna) and the case when a loaded dipole antenna is present inside the enclosure are shown in Fig.10. It can be seen that, especially in some frequency ranges, the presence of the dipole antenna strongly underestimates the level of the SE of the enclosure.

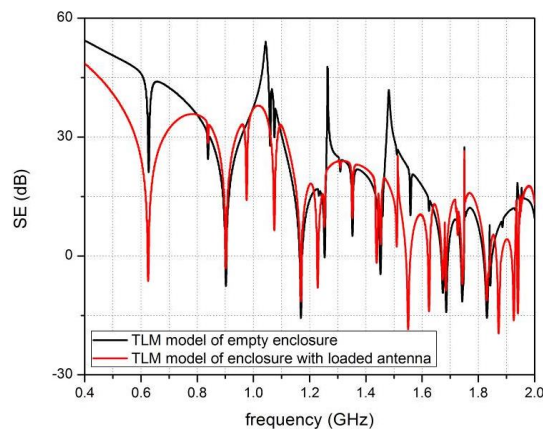


**Fig. 10** SE of enclosure with three  $(10 \times 50)$  mm<sup>2</sup> apertures on the front wall and incident plane wave with azimuth angle  $60^\circ$ , elevation angle  $90^\circ$  and polarization angle  $30^\circ$  - TLM models of enclosure without antenna and with loaded antenna

The physical presence of the coaxial cable inside the enclosure and its impact on the SE is considered next. A coaxial cable of length 140 mm is placed along the  $x$  direction in order to transfer the signal picked up from the center of the dipole receiving antenna to the network analyzer. The radius of outer conductor of coaxial cable is chosen to be equal to the radius of the dipole receiving antenna. For a plane wave of normal incidence to the frontal panel with apertures and with horizontal electric polarization ( $E_y$ ), the presence of the coaxial cable does not have any influence on the SE of enclosure as the dominant EM field component is in the  $y$  direction, while the cable is running in the  $x$  direction. Therefore the SE of the enclosure is the same as shown in Fig. 5 for the TLM model of enclosure with loaded antenna. However, for an obliquely incident plane wave with the

azimuth angle  $60^\circ$ , elevation angle  $90^\circ$  and polarization angle  $30^\circ$ , the coaxial cable has some impact on the SE of enclosure (Fig. 11) as some small current, induced by the  $x$  component of EM field excited inside the enclosure, is running along the cable. It can be seen that the result for the SE of enclosure obtained by using the TLM model with the antenna and cable slightly differs from the SE results calculated by using the TLM model of the enclosure with the loaded antenna. The difference is noticeable at the frequencies where induced current running along the cable is not negligible and therefore enhancing the detected level of  $x$  component of EM field.

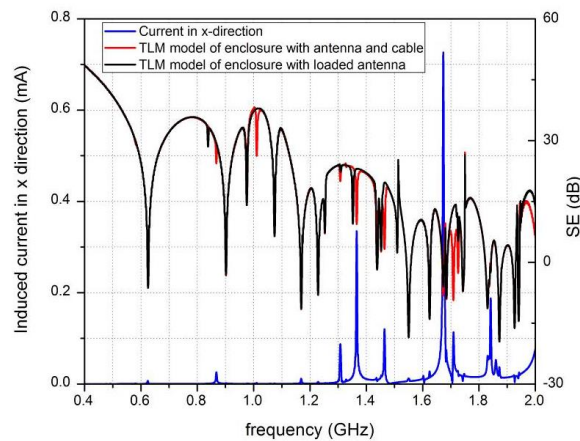


**Fig. 11** SE of enclosure with three  $(10 \times 50)$  mm<sup>2</sup> apertures on the front wall and incident plane wave with azimuth angle  $60^\circ$ , elevation angle  $90^\circ$  and polarization angle  $30^\circ$  - TLM models of enclosure with loaded antenna, with antenna and cable and current induced in the cable

#### 4. CONCLUSION

In this paper, the TLM method with wire node model is used to describe a dipole-receiving antenna and a coaxial cable inside the enclosure and their two-way interaction with EM field. Numerical model follows the experimental arrangement for SE measurements. It is shown that the antenna/cable, in the presence of monitoring EM field, both can have an impact on the measured level of the SE and measured values of resonant frequencies of the enclosure. The level of their impact depends on antenna radius and length but also on cable orientation and external interference incident angle and polarization. Based on these results, authors will be continue their research regarding the impact of different types of monitoring antennas (dipole, monopole, loop) on the EM field distribution inside the protective enclosure and will try to extend the described numerical model taking into consideration the characteristics of balun placed between antenna and cable.

**Acknowledgement:** *This work has been partially supported by the Ministry for Education, Science and Technological Development of Serbia, project number TR32052.*

## REFERENCES

- [1] C. Christopoulos, *Principles and Techniques of Electromagnetic Compatibility*, CRC Press, 2007.
- [2] H. A. Mendez, "Shielding Theory of Enclosures with Apertures", *IEEE Trans. Electromagn. Compat.*, vol. 20, no. 2, pp. 296–305, 1978.
- [3] M.P. Robinson, T. M. Benson, C. Christopoulos, J.F. Dawson, M.D. Ganley, A.C. Marvin, S.J. Porter, D.W.P. Thomas, "Analytical Formulation for the Shielding Effectiveness of Enclosures with Apertures", *IEEE Trans. Electromagn. Compat.*, vol. 40, no. 3, pp. 240–248, 1998.
- [4] J. Shim, D.G. Kam, J.H. Kwon, J. Kim, "Circuitual Modeling and Measurement of Shielding Effectiveness against Oblique Incident Plane Wave on Apertures in Multiple Sides of Rectangular Enclosure", *IEEE Trans. Electromagn. Compat.*, vol. 52, no. 3, pp. 566–577, 2010.
- [5] L.J. Nuebel, J. L. Drewniak, R. E. DuBroff, T.H. Hubing, T. P. Van Doren, "EMI from Cavity Modes of Shielding Enclosures – FDTD Modeling and Measurements", *IEEE Trans. Electromagn. Compat.*, vol. 42, no. 1, pp. 29–38, 2000.
- [6] S. Ali, D.S. Weile, T. Clupper, "Effect of Near Field Radiators on the Radiation Leakage through Perforated Shields", *IEEE Trans. Electromagn. Compat.*, vol. 47, no. 2, pp. 367–373, 2005.
- [7] B.L. Nie, P.A. Du, Y.T. Yu, Z. Shi, "Study of the Shielding Properties of Enclosures With Apertures at Higher Frequencies Using the Transmission-Line Modeling Method", *IEEE Trans. Electromagn. Compat.*, vol. 53, no. 1, pp. 73–81, 2011.
- [8] N. Doncov, B. Milovanović, Z. Stankovic, "Extension of Compact TLM Air-Vent Model on Rectangular and Hexagonal Apertures", *Applied Computational Electromagnetic Society (ACES) journal*, vol. 26, no. 1, pp. 64–72, 2011.
- [9] A. Mallic, D. P. Johns, A. J. Wlodarczyk, "TLM Modelling of Wires and Slots", In Proceedings of International Zurich Symposium on Electromagnetic Compatibility, Zurich, Switzerland, pp. 515–520, 1993.
- [10] V. Milutinovic, T. Cvetkovic, N. Doncov, B. Milovanovic, "Analysis of Enclosure Shielding Properties Dependence on Aperture Spacing and Excitation Parameters", In Proceedings of the IEEE TELSIKS Conference, Niš, Serbia, vol. 2, pp. 521–524, 2011.
- [11] T. Cvetković, V. Milutinović, N. Dončov, B. Milovanović, "TLM modelling of receiving dipole antenna impact on shielding effectiveness of enclosure", *Int. J. Reasoning-based Intelligent Systems*, vol. 5, no. 3, pp. 202–207, 2013.
- [12] V. Milutinović, T. Cvetković, N. Dončov, B. Milovanović, "Circuitual and Numerical Models for Calculation of Shielding Effectiveness of Enclosure with Apertures and Monitoring Dipole Antenna Inside", *Radioengineering*, vol. 22, no. 4, pp 1249–1257, 2013.
- [13] T. Cvetković, V. Milutinović, N. Dončov, B. Milovanović, "Numerical Investigation of Monitoring Antenna Influence on Shielding Effectiveness Characterization", *Applied Computational Electromagnetic Society (ACES) Journal*, vol. 29, no. 11, pp 837–845, 2014.
- [14] J. Jokovic, B. Milovanovic, N. Doncov, "Numerical Model of Transmission Procedure in a Cylindrical Metallic Cavity Compared with Measured Results", *Int. Journal of RF and Microwave Computer-Aided Engineering*, vol. 18, no. 4, pp. 295–302, 2008.
- [15] A.J. Wlodarczyk, V. Trenkic, R. Scaramuzza, C. Christopoulos, "A Fully Integrated Multiconductor Model for TLM", *IEEE Trans. Microwave Theory Tech.*, vol. 46, no. 12, pp. 2431–2437, 1998.
- [16] T. Dimitrijevic, J. Jokovic, B. Milovanovic, N. Doncov, "TLM Modeling of a Probe-Coupled Cylindrical Cavity Based on Compact Wire Model in the Cylindrical Mesh", *Int. Journal of RF and Microwave Computer-Aided Engineering*, vol. 22, no. 2, pp. 184–192, 2012.
- [17] C. Christopoulos, *The Transmission-Line Modelling (TLM) Method*, IEEE/OUP Series, Piscataway, NJ, 1995.